

Epitaxial structure and transport in LaTiO_{3+x} films on (001) SrTiO_3

K. H. Kim¹, D. P. Norton^{*1}, J. D. Budai², M. F. Chisholm², B. C. Sales², D. K. Christen², and C. Cantoni²

¹ University of Florida, Dept. of Materials Science and Engineering, 106 Rhines Hall, Gainesville, 32611 USA

² Oak Ridge National Laboratory, Oak Ridge, 37831 USA

Received 20 May 2003, accepted 6 August 2003

Published online 14 November 2003

PACS 61.10.Nz, 68.37.Lp, 68.55.Jk, 73.61.Le

The structure and transport properties of LaTiO_{3+x} epitaxial thin films grown on (001) SrTiO_3 by pulsed-laser deposition is examined. Four-circle X-ray diffraction indicates that the films possess the defect perovskite LaTiO_3 structure when deposited in vacuum, with the higher X compounds forming at moderate oxygen pressures. The crystal structure of the LaTiO_3 films is tetragonal in the epitaxial films, in contrast to the orthorhombic structure observed in bulk materials. A domain structure is observed in the films, consisting of LaTiO_3 oriented either with the [110] or [001] directions perpendicular to the substrate surface. Z-contrast scanning transmission electron microscopy reveals that this domain structure is not present in the first few unit cells of the film, but emerges approximately 2–3 nm from the $\text{SrTiO}_3/\text{LaTiO}_3$ interface. Upon increasing the oxygen pressure during growth, a shift in the lattice d-spacing parallel to the substrate surface is observed, and is consistent with the growth of the $\text{La}_2\text{Ti}_2\text{O}_7$ phase. However, van der Pauw measurements show that the films with the larger d-spacing remain conductive, albeit with a resistivity that is significantly higher than that for the perovskite LaTiO_3 films. The transport behavior suggests that the films grown at higher oxygen pressures are LaTiO_{3+x} with $0.4 < x < 0.5$.

© 2003 WILEY-VCH Verlag GmbH & Co. KGaA, Weinheim

The fundamental properties and potential applications of conducting oxides are of significant interest [1–3]. Among the materials investigated is the (La, Sr) TiO_{3+x} system [4–10]. LaTiO_{3+x} is an interesting defect perovskite, with transport properties varying from insulating to metallic based on oxygen stoichiometry. These materials can be viewed as members of a homologous series $\text{A}_{n+1}\text{B}_{n+1}\text{O}_{3n+5}$, where $n = \infty$ is LaTiO_3 . At room temperature, LaTiO_3 possesses the orthorhombic GdFeO_3 perovskite structure with $a = 5.604 \text{ \AA}$, $b = 5.595 \text{ \AA}$, and $c = 7.906 \text{ \AA}$ [11]. LaTiO_3 is a Mott insulator with a G-type antiferromagnetic ordered ground state and a Néel temperature of approximately 135 K. LaTiO_3 is a semiconductor at high temperature, becoming an antiferromagnetic insulator upon cooling through the Néel temperature. When synthesized with moderate oxygen content, LaTiO_{3+x} is metallic at high temperature, with a metal-insulator transition occurring at reduced temperature. For $0.1 < x < 0.2$, the material is metallic at all temperatures and is structurally viewed as a disordered perovskite. At $x = 0.2$, bulk samples show phase separation, resulting in a disordered intergrowths of the perovskite and a laminar structure. At $x = 0.4$, an ordered monoclinic phase, $\text{La}_5\text{Ti}_5\text{O}_{17}$, has been observed with $a = 7.86 \text{ \AA}$, $b = 5.53 \text{ \AA}$, $c = 31.5 \text{ \AA}$, and $\beta = 97.2^\circ$ [9]. This phase can be viewed as a 2D layered structure consisting of perovskite slabs connected by La cations. Transport measurements on bulk samples indicate that $\text{LaTiO}_{3.4}$ is a p-type semiconductor. For $x = 0.5$, the material becomes ferroelectric, assuming the mono-

* Corresponding author: e-mail: dnort@mse.ufl.edu

© 2003 WILEY-VCH Verlag GmbH & Co. KGaA, Weinheim

clinic $\text{La}_2\text{Ti}_2\text{O}_7$ layered structure made of two regular perovskite units stacked between two distorted units that share an additional oxygen layer. $\text{La}_2\text{Ti}_2\text{O}_7$ exhibits a relatively high Curie temperature of 1773 K [12]. The saturation polarization is $5 \mu\text{C}/\text{cm}^2$, and the coercive field is 45 kV/cm. Upon doping with Sr, bulk $\text{La}_{1-x}\text{Sr}_x\text{TiO}_3$ transforms from an antiferromagnetic p-type semiconductor to an n-type metal [13–15]. The crystal structure remains orthorhombic $Pbnm$ up to $x = 0.3$, where it becomes orthorhombic $Ibmm$. For $x > 0.7$, bulk $\text{La}_{1-x}\text{Sr}_x\text{TiO}_3$ becomes cubic.

Epitaxial film growth studies have explored the LaTiO_{3+x} and $(\text{La,Sr})\text{TiO}_3$ system [16–20]. Using molecular beam epitaxy, it has been shown that phase formation in the LaTiO_x system can be controlled via selection of oxidation conditions and temperature during growth. Pulsed-laser deposition studies suggest that only two phases, namely LaTiO_3 and $\text{La}_2\text{Ti}_2\text{O}_7$, occur in thin films [17]. The epitaxial growth of $(\text{La,Sr})\text{TiO}_3$ thin films has also been examined using pulsed-laser deposition. $\text{La}_{0.5}\text{Sr}_{0.5}\text{TiO}_3$ films have been realized with resistivity on the order to $60 \mu\Omega\text{-cm}$ at room temperature [20]. Interestingly, epitaxial $\text{La}_{0.5}\text{Sr}_{0.5}\text{TiO}_3$ thin films have also been realized that are reasonably transparent and conductive [21]. In this case, films with a resistivity of $\sim 350 \mu\Omega\text{-cm}$ were measured to possess a transparency of $\sim 70\%$ over the visible wavelengths. As a metallic oxide, $(\text{La,Sr})\text{TiO}_3$ is being considered for numerous applications, including conducting electrodes for ferroelectrics [22] and dielectric-base transistors [23], as well as for sensors [24]. Another potential application of $(\text{La,Sr})\text{TiO}_3$ is in the development of coated conductors based on epitaxial high temperature superconducting (HTS) films deposited on metal tapes [25, 26].

In this paper, we examine the properties of LaTiO_{3+x} epitaxial films on SrTiO_3 , focusing on the crystallographic and transport properties as a function of the deposition conditions. The pseudo-cubic lattice parameter for LaTiO_3 of 3.96 \AA provides a relatively small lattice mismatch to SrTiO_3 ($a = 3.905 \text{ \AA}$). The conductivity of LaTiO_3 films is measured and correlated with the structure. The growth of LaTiO_3 thin films was achieved using pulsed-laser deposition. A KrF (248 nm) excimer laser was used as the ablation source. Laser energy densities on the order of $1\text{--}3 \text{ J}/\text{cm}^2$ were utilized. Films were deposited at temperatures ranging from $500\text{--}770 \text{ }^\circ\text{C}$ in pressures ranging from vacuum (10^{-6} T) to oxygen partial pressures of 10^{-2} T . Polycrystalline LaTiO_3 targets were used as the ablation materials. Total deposition time was 0.5 to 1 hr with a laser repetition rate of 5 Hz. In most cases, the films were rapidly cooled in the growth pressure following deposition. Single crystal (001) SrTiO_3 was used as the substrate material. The transport and structural properties of the LaTiO_{3+x} thin films were then characterized. Transport was determined at room temperature using a van der Pauw configuration. X-ray diffraction was used to determine crystallographic orientation and lattice spacing. Z-contrast scanning transmission electron microscopy (Z-STEM) was also employed to examine the structure of the films.

Using pulsed-laser deposition, epitaxial structures were grown on (001) SrTiO_3 . Four-circle X-ray diffraction was used to characterize the crystallinity and orientation of the films. Figure 1 shows a low-resolution $\theta\text{--}2\theta$ scan along the SrTiO_3 (001) for a LaTiO_3 film on SrTiO_3 . Note that the diffraction peaks are very close to the substrate (00 l) peaks. Figure 2a shows a X-ray diffraction ϕ -scan through the LaTiO_3 (112), showing that the film is epitaxial on the (001) SrTiO_3 surface. The in-plane mosaic is $\Delta\phi \sim 2^\circ$. Figure 2b shows the out-of-plane rocking curve, yielding a mosaic spread of $\Delta\theta \sim 1.3^\circ$. Based on the in-plane and high-resolution scans, the LaTiO_3 film could be indexed as possessing two orienta-

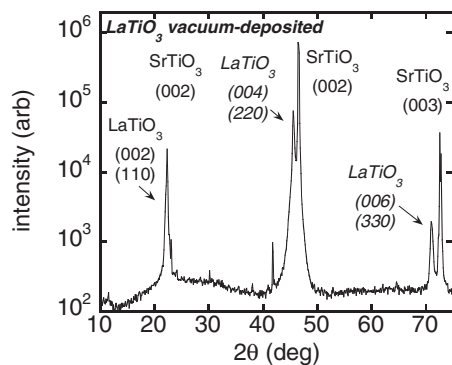


Fig. 1 X-ray diffraction $\theta\text{--}2\theta$ scans taken along the surface normal for a LaTiO_3 film deposited on (001) SrTiO_3 at 10^{-6} T and $750 \text{ }^\circ\text{C}$ using pulsed laser deposition.

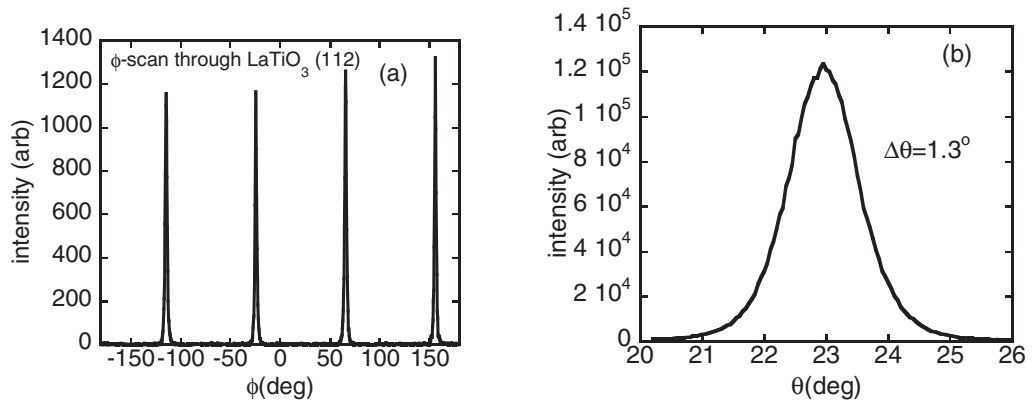


Fig. 2 X-ray diffraction a) ϕ -scan and b) out-of-plane rocking curve taken of a LaTiO_3 film deposited on (001) SrTiO_3 at 10^{-6} T and 750°C using pulsed laser deposition.

tions, namely domains with the LaTiO_3 (110) perpendicular to the substrate surface or domains with the LaTiO_3 (001) perpendicular. Note that there was no evidence of an orthorhombic a, b splitting as has been reported for the bulk. If the peaks along the surface normal are indexed as LaTiO_3 (001) perpendicular, then the resulting tetragonal lattice parameters are $a = b = 5.594 \text{ \AA}$, $c = 7.880 \text{ \AA}$. For this orientation, the out-of-plane LaTiO_3 [001] is along the SrTiO_3 [001], while the in-plane LaTiO_3 [001] is along the SrTiO_3 [110]. Alternatively, if the peaks along the surface normal are indexed as (110) perpendicular, then $a = b = 5.572 \text{ \AA}$, $c = 7.910 \text{ \AA}$. For this orientation, the out-of-plane LaTiO_3 [110] is along the SrTiO_3 [001], while the in-plane LaTiO_3 [001] is along the SrTiO_3 [100]. Note that the two sets of lattice values are related by interchanging (a, b) with c and scaling by $\sqrt{2}$. Both of these orientations exist in the film with comparable volume fraction. This is evident in that the LaTiO_3 (111) peak is observed at two different χ positions (angle from surface normal) as seen in Fig. 3. Thus, the LaTiO_3 films are twinned, consisting of two distinct domains.

The interface and twin structure were further examined using Z-STEM. Figure 4 shows the (Z-STEM) image of an epitaxial $\text{LaTiO}_3/\text{SrTiO}_3$ interface grown at 750°C in vacuum. Note that the first few unit cells of LaTiO_3 grown on the (001) SrTiO_3 surface are untwinned, indicating an epitaxial stabilization of the perovskite phase. However, as the layer thickness exceeds ~ 3 unit cells, twinning is observed in the LaTiO_{3+x} , indicating a relaxation of strain and the formation of a domain structure. This is consistent with the X-ray diffraction data, showing two distinct orientations for the film grains.

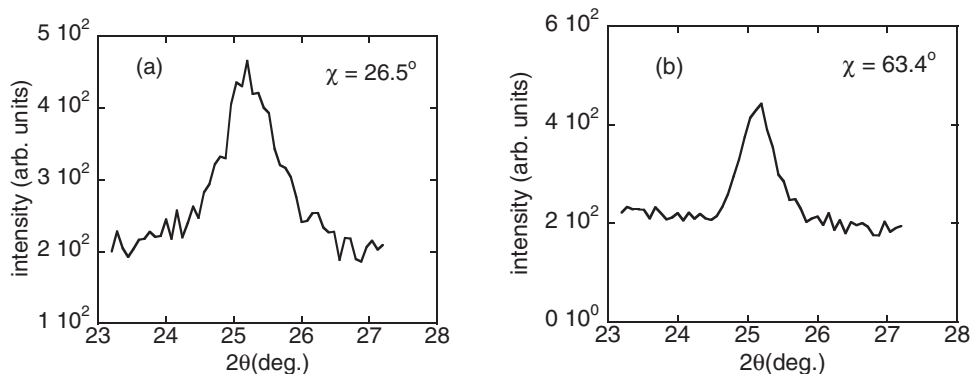


Fig. 3 X-ray diffraction scan of the LaTiO_3 (111) taken at χ values of a) 26.5° and b) 63.4° for a LaTiO_3 film deposited on (001) SrTiO_3 at 10^{-6} T and 750°C using pulsed laser deposition.

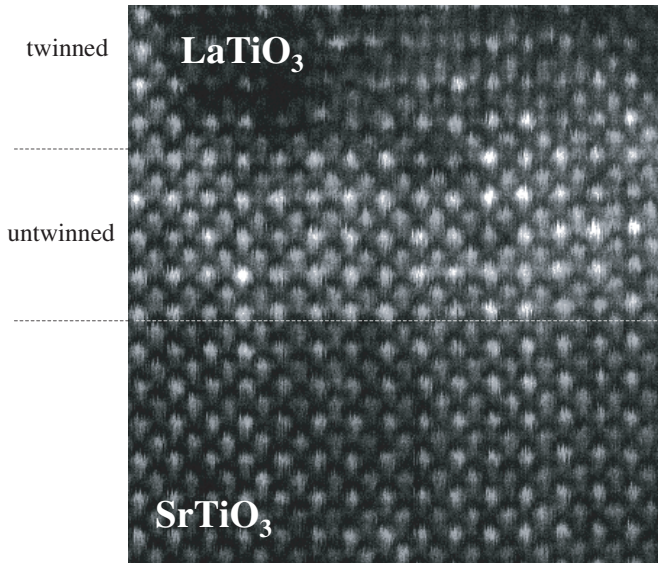


Fig. 4 Z-contrast STEM image of a SrTiO₃/LaTiO₃ interface showing twin formation.

As reported for bulk materials, the structural and transport properties of the LaTiO_{3+x} films depend strongly on the oxidizing environment utilized during growth. Figure 5a shows the X-ray diffraction data from the θ - 2θ scan for LaTiO_{3+x} films grown at 700 °C in an oxygen pressure of 10⁻³ T. Here, the film diffraction peaks for lattice planes parallel to the substrate surface clearly shift to lower angle as the oxygen pressure during growth is increased from vacuum to only 10⁻³ T. Figure 5b shows the shift in the low-angle peak as O₂ is increased during growth. This data indicates a discontinuous change in *d*-spacing from 3.98 Å for films deposited in vacuum to 4.20 Å for films deposited at 10⁻³ T. Previous studies of epitaxial LaTiO_{3+x} films have assigned this shift in *d*-spacing to the growth of the La₂Ti₂O₇ phase [17]. The phase progression from LaTiO₃ to LaTiO_{3.5} involves the insertion of an oxygen intergrowth along the original perovskite (110) plane.

In addition to structure, we have also measured the transport properties of the LaTiO_{3+x} films as a function of oxygen pressure during growth. As oxygen pressure is moderately increased, the resistivity of the deposited films increases rapidly. The transport behavior of epitaxial LaTiO₃ films grown on SrTiO₃ is indicated in Fig. 6, where the room temperature resistivity is plotted as a function of oxygen

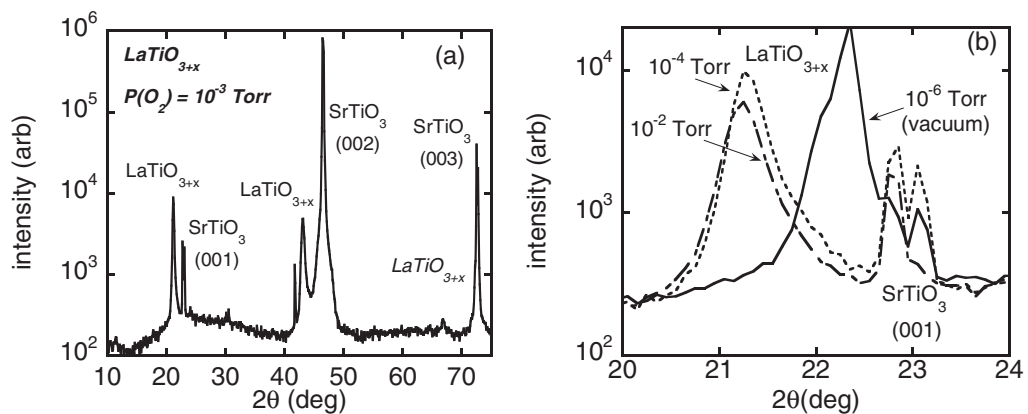


Fig. 5 X-ray diffraction θ - 2θ scan taken along the surface normal for LaTiO_{3+x} film deposited at 750 °C on (001) SrTiO₃ at a) 10⁻³ T oxygen pressure. Also shown b) are the diffraction peaks at low angles, indicating the shift in *d*-spacing with the introduction of oxygen during film growth.

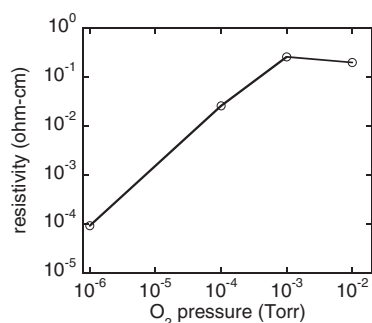


Fig. 6 Resistivity for LaTiO_{3+x} films grown on (001) SrTiO_3 at various oxygen pressures.

pressure during growth. For films grown in vacuum, the resistivity is low, on the order of $10^{-4} \Omega \text{ cm}$. This is consistent with the formation of the LaTiO_3 perovskite phase. As the oxygen partial pressure is increased to 10^{-4} T , the resistivity of the LaTiO_{3+x} film increases by more than two orders of magnitude to $\sim 0.026 \Omega \text{ cm}$. At 10^{-3} T , the resistivity is $0.26 \Omega \text{ cm}$. This increase in resistivity with oxygen pressure during growth coincides with a structural transition as is evident in the X-ray diffraction patterns shown in Fig. 5. However, the transport properties do not agree with the formation of stoichiometric $\text{La}_2\text{Ti}_2\text{O}_7$ as this should be an insulating ferroelectric. Instead, the films are semiconducting, which is more consistent with films with $0.4 < x < 0.5$.

In conclusion, we have investigated the transport and structural properties of LaTiO_{3+x} epitaxial thin films grown by pulsed laser deposition. These results show that LaTiO_3 thin films exhibit a domain structure with a tetragonal structure. The transport properties are sensitive to the oxidation conditions during growth.

Acknowledgement This work was supported through a contract with Oak Ridge National Laboratory, which is managed by UT/Battelle under U.S. Government contract DE-AC05-00OR22725, as well as from the Air Force Office of Scientific Research.

References

- [1] D. S. Ginley and C. Bright, *MRS Bull.* **25**, 15 (2000).
- [2] J. B. Goodenough, "Metallic Oxides", in *Progress in Solid State Chemistry* 5, (Pergamon Press, Oxford, 1971) pp. 145–399.
- [3] P. A. Cox, "Transition Metal Oxides", (Clarendon Press, Oxford, 1995).
- [4] Y. Tokura, *Physica B* **237–238**, 1 (1997).
- [5] G. Khaliullin and S. Maekawa, *Phys. Rev. Lett.* **85**, 3950 (2000).
- [6] B. Keimer, D. Casa, A. Ivanov, J. W. Lynn, M. v. Zimmermann, J. P. Hill, D. Gibbs, Y. Taguchi, and Y. Tokura, *Phys. Rev. Lett.* **85**, 3946 (2000).
- [7] J. G. Bednorz, *Physica C* **282–287**, 37 (1997).
- [8] S. Miyahara and F. Mila, *Progress of Theoretical Physics Supplement*, Issue **145**, 266 (2002).
- [9] F. Lichtenberg, D. Widmer, J. G. Bednorz, T. Williams, and A. Reller, *Z. Phys. B, Condens. Matter* **82**, 211 (1991).
- [10] T. Williams, F. Lichtenberg, D. Widmer, J. G. Bednorz, and A. Reller, *J. Solid State Chem.* **103**, 375 (1993).
- [11] K. Yoshii, A. Nakamura, and H. Abe, *J. Alloys and Compd.* **290**, 236 (1999).
- [12] S. Nanamatsu, M. Kimura, K. Doi, S. Matsushita, and N. Yamada, *Ferroelectrics* **8**, 511 (1974).
- [13] C. C. Hays, J. S. Zhou, J. T. Markert, and J. B. Goodenough, *Phys. Rev. B* **60**, 10367 (1999).
- [14] Y. Tokura, Y. Taguchi, Y. Okada, Y. Fujishima, T. Arima, K. Kumagai, and Y. Iye, *Phys. Rev. Lett.* **70**, 2126 (1993).
- [15] Y. Maeno, S. Awaji, H. Matsumoto, and T. Fujita, *Physica B* **165–166**, Part 2, 1185 (1990).
- [16] J. W. Seo, J. Fompeyrine, H. Siegwart, and J.-P. Locquet, *Phys. Rev. B* **63**, 205401/1–7 (2001).
- [17] A. Ohtomo, D. A. Muller, J. L. Grazul, and H. Y. Hwang, *Appl. Phys. Lett.* **80**, 3922 (2002).
- [18] S. Gariglio, J. W. Seo, J. Fompeyrine, J.-P. Locquet, and J.-M. Triscone, *Phys. Rev. B* **63**, 161103/1–4 (2001).
- [19] C. Yoshida, H. Tamura, A. Yoshida, Y. Kataoka, N. Fujimaki, and N. Yokoyama, *Jap. J Appl. Phys.* **35**, 5691 (1996).

- [20] W. Wu, F. Lu, K. H. Wong, G. Pang, C. L. Choy, and Y. Zhang, *J. Appl. Phys.* **88**, 700 (2000).
- [21] J. H. Cho and H. J. Cho, *Appl. Phys. Lett.* **79**, 1426 (2001).
- [22] B. T. Liu, K. Maki, Y. So, V. Nagarajan, R. Ramesh, J. Lettieri, J. H. Haeni, D. G. Schlom, W. Tian, X. Q. Pan, F. J. Walker, and R. A. McKee, *Appl. Phys. Lett.* **80**, 4801 (2002).
- [23] T. Hato, A. Yoshida, C. Yoshida, H. Suzuki, and N. Yokoyama, *Appl. Phys. Lett.* **70**, 2900 (1997).
- [24] G. Q. Li, P. T. Lai, S. H. Zeng, M. Q. Huang, and Y. C. Cheng, *Sens. Actuators A* **63**, 223 (1997).
- [25] D. P. Norton, A. Goyal, J. D. Budai, D. K. Christen, D. M. Kroeger, E. D. Specht, Q. He, B. Saffian, M. Paranthaman, C. Klabunde, D. F. Lee, B. C. Sales, and F. A. List, *Science* **274**, 755 (1996).
- [26] X. D. Wu, S. R. Foltyn, P. N. Arendt, W. R. Blumenthal, I. H. Campbell, J. D. Cotton, J. Y. Coulter, W. L. Hulls, M. P. Maley, H. F. Safar, and J. L. Smith, *Appl. Phys. Lett.* **67**, 2397 (1995).